

# UC Irvine

## UC Irvine Previously Published Works

### Title

Different Time Evolution of Oxyhemoglobin and Deoxyhemoglobin Concentration Changes in the Visual and Motor Cortices during Functional Stimulation: A Near-Infrared Spectroscopy Study

### Permalink

<https://escholarship.org/uc/item/8bw3h4cs>

### Journal

NeuroImage, 16(3)

### ISSN

1053-8119

### Authors

Wolf, Martin  
Wolf, Ursula  
Toronov, Vlad  
et al.

### Publication Date

2002-07-01

### DOI

10.1006/nimg.2002.1128

### Copyright Information

This work is made available under the terms of a Creative Commons Attribution License, available at <https://creativecommons.org/licenses/by/4.0/>

Peer reviewed

# Different Time Evolution of Oxyhemoglobin and Deoxyhemoglobin Concentration Changes in the Visual and Motor Cortices during Functional Stimulation: A Near-Infrared Spectroscopy Study

Martin Wolf, Ursula Wolf, Vlad Toronov, Antonios Michalos, L. Adelina Paunescu,  
Jee Hyun Choi, and Enrico Gratton

Laboratory for Fluorescence Dynamics, Department of Physics, University of Illinois at Urbana-Champaign,  
1110 W. Green St., Urbana, Illinois 61801-3080

Received August 10, 2001

Neurovascular coupling is the generic term for changes in cerebral metabolic rate of oxygen (CMRO<sub>2</sub>), cerebral blood flow, and cerebral blood volume related to brain activity. The goal of this paper is to better understand the effects of neurovascular coupling in the visual and motor cortices using frequency-domain near-infrared spectroscopy. Maps of concentration changes in oxyhemoglobin [O<sub>2</sub>Hb], deoxyhemoglobin [HHb], and total hemoglobin of the visual and motor cortices were generated during stimulation using a reversing checkerboard screen and palm-squeezing, respectively. Seven healthy volunteers of 18–37 years of age were included. In the visual cortex the patterns of [O<sub>2</sub>Hb] and [HHb] were strongly linearly correlated ( $r^2 > 0.8$  in 13 of a total of 24 locations). In 20 locations the change in [O<sub>2</sub>Hb] was larger than 0.25  $\mu$ M. The mean slope of the linear regression between [O<sub>2</sub>Hb] and [HHb] was  $-3.93 \pm 0.31$  (SE). The patterns of the [O<sub>2</sub>Hb] and [HHb] traces over the motor cortex looked different. The [O<sub>2</sub>Hb] reached its maximum change a few seconds before the [HHb] reached its minimum. This was confirmed by the linear regression analysis ( $r^2 > 0.8$  in none of 40 locations). In 20 locations the change in [O<sub>2</sub>Hb] was larger than 0.25  $\mu$ M. The mean slope of the regression line was  $-1.76 \pm 0.20$ , which is significantly higher than that in the motor cortex ( $P < 0.0000001$ ). Patterns of [O<sub>2</sub>Hb] and [HHb] differ among cortex areas. This implies that the regulation of perfusion in the visual cortex is different from that in the motor cortex. There is evidence that the CMRO<sub>2</sub> increases substantially in the visual cortex, while this is not the case for the motor cortex. © 2002 Elsevier

Science (USA)

**Key Words:** near-infrared spectroscopy; visual cortex; motor cortex; stimulation; oxyhemoglobin; deoxyhemoglobin; neurovascular coupling.

## INTRODUCTION

Neurovascular coupling is the generic term for changes in cerebral metabolic rate of oxygen (CMRO<sub>2</sub>), cerebral blood flow (CBF), and cerebral blood volume (CBV) related to brain activity (Frostig *et al.*, 1990; Maki *et al.*, 1995; Villringer and Dirnagl, 1995). The goal of this paper is to better understand the effects of neurovascular coupling.

In recent years several techniques have been applied to determine these parameters during functional brain activation, where the parameters are either measured directly or calculated from other measurands. Magnetic resonance imaging (MRI) measures CBF and CBV using a contrast agent (Wirestam *et al.*, 2000). With positron emission tomography, CMRO<sub>2</sub> and CBF can be determined (Meltzer *et al.*, 2000). While both techniques provide an excellent spatial resolution on the order of millimeters, continuous monitoring is not possible due to its relatively low time resolution (s) and the requirement of the application of a contrast agent. MRI directly determines changes in deoxyhemoglobin concentration [HHb] through the blood oxygen level-dependent (BOLD) signal with a high time ( $\sim 0.5$ -s) and spatial ( $\sim 0.5$ -cm) resolution. However, changes in [HHb] are not measured quantitatively and they do not provide any information on oxyhemoglobin concentration [O<sub>2</sub>Hb]. Near-infrared spectroscopy (NIRS), due to its high time resolution (ms) and good spatial resolution (cm) offers the option of continuously recording changes of physiological parameters during brain activation. Due to this and its other advantageous features such as noninvasiveness, the capability to be performed at bedside, the absence of ionizing radiation, and the relatively low cost, it has been increasingly used in brain research (Hoshi *et al.*, 1994; Villringer and Chance, 1997). It detects changes in [O<sub>2</sub>Hb] and [HHb] and therefore total hemoglobin ([tHb]), which corresponds to CBV. In addition to the change in the

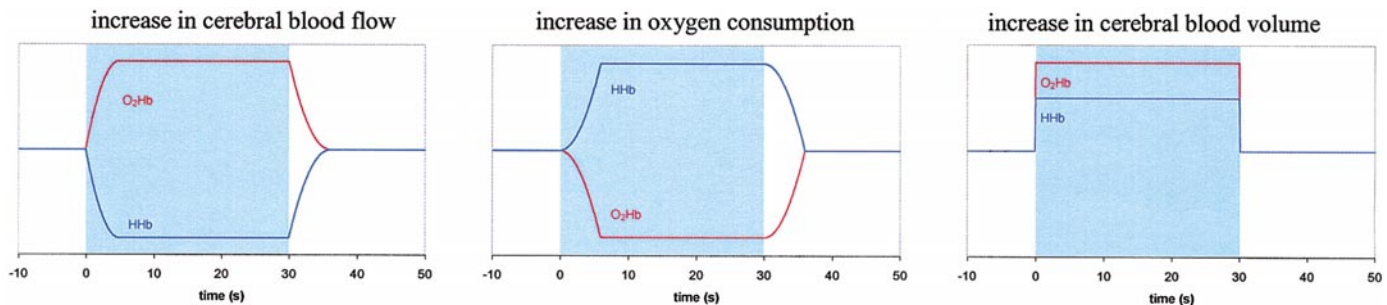


**FIG. 1.** The effect of an isolated increase in cerebral blood flow (left), cerebral metabolic rate of oxygen (middle), or total hemoglobin concentration (right) on the time evolution of the  $[O_2Hb]$  and  $[HHb]$  as predicted by the one-compartment model. The shaded area indicates the period when the respective parameter is increased. Increases in cerebral blood flow or cerebral metabolic rate of oxygen produce symmetric patterns, which is not the case for an increase in total hemoglobin concentration. The latter also depends on the oxygen saturation of the additional hemoglobin.

CBV the changes in CBF and  $CMRO_2$  also affect the  $[O_2Hb]$  and  $[HHb]$  traces (Mayhew *et al.*, 2000). Considering the following theoretical implications, the influence of CBV, CBF, and  $CMRO_2$  on the  $[O_2Hb]$  and  $[HHb]$  traces can be demonstrated.

Assuming a one-compartment model, an isolated change in CBF (Fig. 1, left) will have the depicted effect on the  $[O_2Hb]$  and  $[HHb]$ . The increase in CBF will lead to an increase in  $[O_2Hb]$  and a decrease in  $[HHb]$  because more oxygenated than deoxygenated blood will fill the compartment. This effect is often described as the washout effect. Note that the changes are completely symmetrical; i.e., the  $[O_2Hb]$  and  $[HHb]$  traces are perfect mirror images.

Figure 1 (middle) shows how an isolated increase in  $CMRO_2$  affects the  $[O_2Hb]$  and  $[HHb]$  in a one-compartment model. If we assume an isolated increase in  $CMRO_2$  the pattern for  $[O_2Hb]$  and  $[HHb]$  looks almost exactly opposite to the pattern of an increase in CBF. The  $[HHb]$  increases because oxygen ( $O_2$ ) is consumed without being replaced. The decrease in  $[O_2Hb]$  is symmetrical to the increase in  $[HHb]$ .

As shown in Fig. 1 (right) an isolated increase in CBV leads to an increase in both  $[O_2Hb]$  and  $[HHb]$ . A change in  $[tHb]$  is the only effect, which leads to asymmetrical changes in  $[O_2Hb]$  and  $[HHb]$ . The amount of change in  $[O_2Hb]$  versus  $[HHb]$  depends on the oxygen saturation of the additional blood.

The goal of this paper is to better understand the effects of the neurovascular coupling on the basis of our NIRS measurements and to test whether the effects are similar in different areas of the human cortex. We investigated two major areas of the human brain cortex during functional stimulation. The protocols included measurements over the visual cortex during visual stimulation and over the motor cortex during a contralateral palm-squeezing task. Maps of the traces for  $[O_2Hb]$ ,  $[HHb]$ , and  $[tHb]$  were generated and analyzed. The results obtained from the visual and motor cortices were compared between each other and to values and patterns reported in the literature.

## MATERIAL AND METHODS

### Instrument

We used a frequency-domain spectrometer (Oximeter, ISS, Champaign, IL, USA) which is described in detail elsewhere (Fantini *et al.*, 1995). In brief, the instrument operates at two different wavelengths, either 758 and 830 nm (motor stimulation) or 670 and 830 nm (visual stimulation). The light generated by 16 laser diodes (8 per wavelength) is intensity-modulated at a frequency of 110 MHz. The light from the instrument to the tissue and back to the instrument is guided through optical fibers. The incoming light is collected in photomultiplier tubes (PMT) and demodulated, and its mean intensity (DC), modulation amplitude (AC), and phase are determined. The output signals from the PMTs are sent to a computer for data processing.

### Sensor

To reach the visual cortex, which lies deeper in the human head due to the anatomical structure, we used

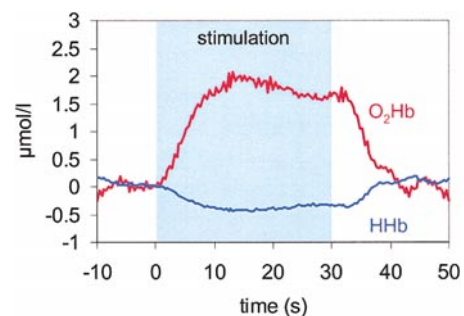
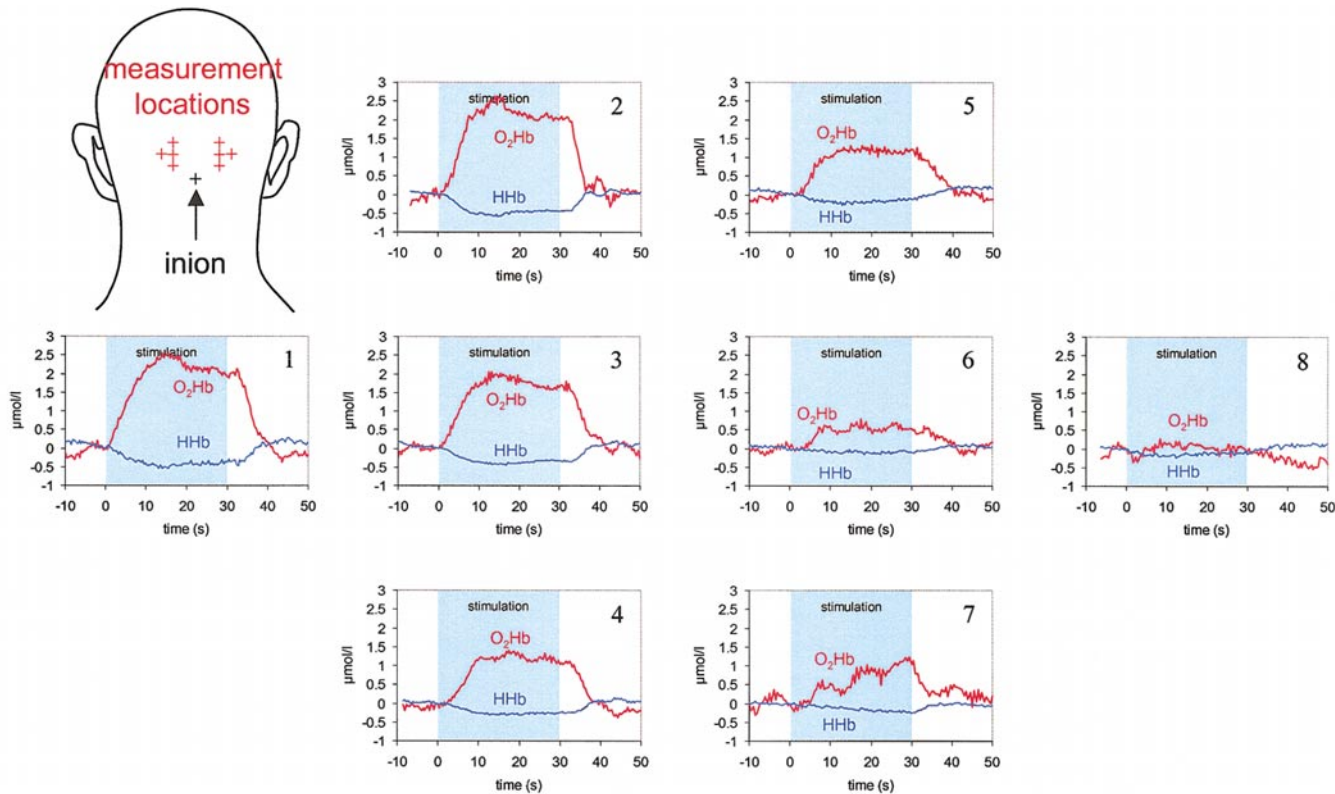


**FIG. 2.** A typical course of the traces of  $[O_2Hb]$  and  $[HHb]$  during neurovascular coupling. After the onset of the stimulation the  $[O_2Hb]$  increases and the  $[HHb]$  decreases until both components reach a plateau. The end of the stimulation is followed by a decrease in  $[O_2Hb]$  and an increase in  $[HHb]$  until they return to baseline. The decrease in  $[HHb]$  is approximately four times smaller than the increase in  $[O_2Hb]$ . The traces were obtained using a folding average of the  $[O_2Hb]$  and  $[HHb]$  responses to 20 repetitive visual stimulation periods in location 3 (see Fig. 3) of subject 2.

3



4

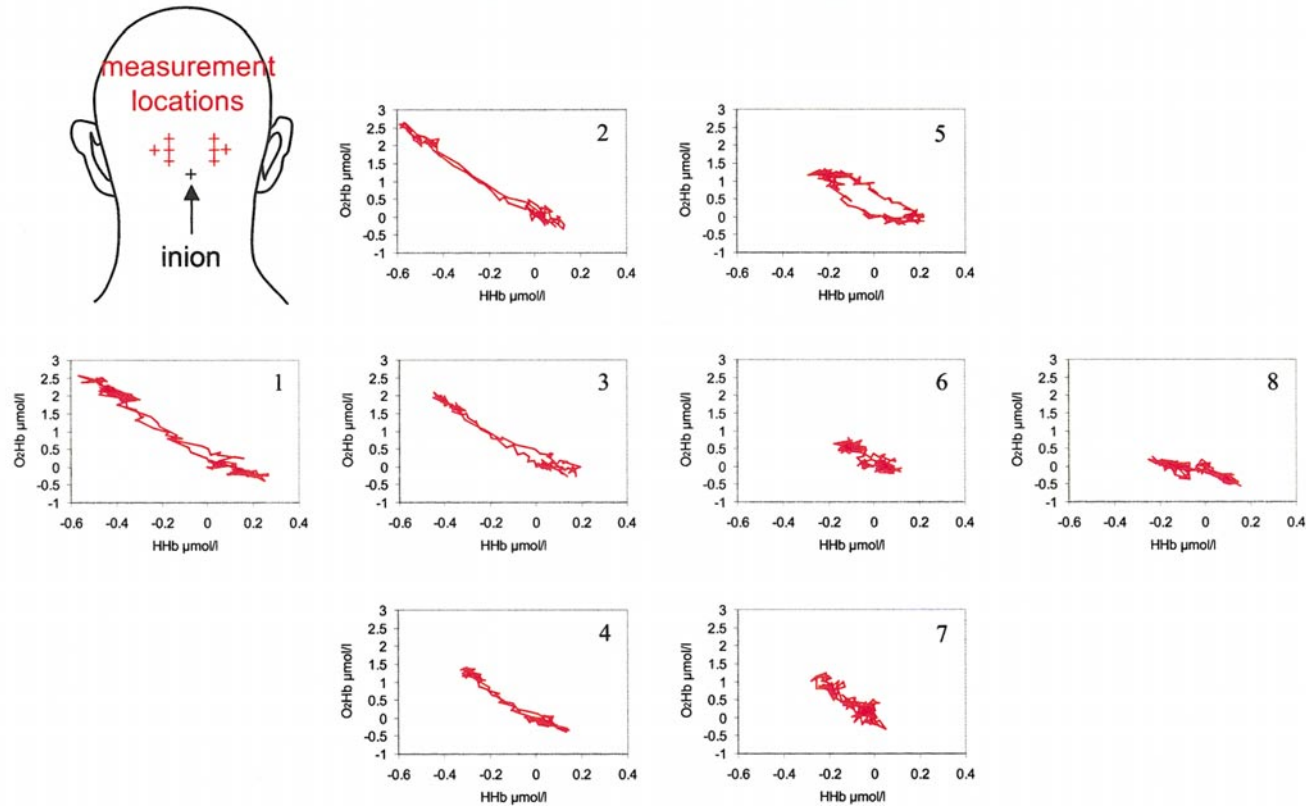


**FIG. 3.** The diagram of the head illustrates the arrangement of the eight locations over the visual cortex and their distances. The bottom cross marks the inion. The graphs represent  $[O_2Hb]$  and  $[HHb]$  traces averaged over 20 visual stimulation periods in subject 2 obtained at the eight locations over the visual cortex. Note that by moving the sensor by only 0.5 cm the signal changes and almost disappears in some instances.

**FIG. 4.** The same traces and locations as in Fig. 3 but  $[HHb]$  traces are plotted versus the  $[O_2Hb]$  traces. Thus a remarkably linear relationship between the two variables is revealed.

a geometry with two crossed source detector pairs where we combined the light of two laser diodes for each wavelength (670 and 830 nm) to achieve a better signal to noise ratio. This geometry had been developed and described by our group earlier (Filiaci *et al.*, 1998). The source-detector distance was 3.5 cm and the probe covered an area of  $2.4 \times 2.4$  cm. Maps were generated by moving the sensor sequentially from location to location over the visual cortex and repeating the measurement.

For probing the motor cortex two detector fibers and eight paired source fibers (758 and 830 nm) were arranged in a geometry to obtain measurements from 10 channels simultaneously. The source detector distance was 3.0 cm and the probe covered an area of  $6 \times 9$  cm.

### Protocols

For both protocols the subjects were placed in a dim quiet room.

**Visual stimulation.** The optodes were placed sequentially at eight different locations (four over each hemisphere) over the visual cortex using theinion as an orientation mark (Kato *et al.*, 1993; Meek *et al.*, 1995). The distance between the locations over one hemisphere was 0.5 cm.

The stimulus was displayed on a checkerboard. The subject was asked to close her/his eyes during the resting periods and to focus on a light-emitting diode in the center of the checkerboard during the stimulation periods. One measurement cycle included three periods: (1) 10 s while the checkerboard was illuminated, (2) 20 s while the checkerboard was reversing, and (3) 30 s rest while the checkerboard was turned off. The entire time when the checkerboard was illuminated is regarded as the functional stimulation. For each location this cycle was repeated 20 times. Preceding the first and following the last stimulation cycle a 2-min baseline was recorded. The reversing frequency of the checkerboard was set to 2.0 or 2.5 Hz depending on the subject's heart rate to avoid pulse harmonics. After completing 20 cycles at one location the sensor was moved to the next position and the measurement repeated.

**Motor stimulation.** The sensor was placed over the left motor cortex (all subjects were right handed) using the C3 position as the orientation mark according to the international electroencephalograph 10/20 system (Steinmetz *et al.*, 1989). Measurements were recorded in all 10 locations simultaneously.

During stimulation periods the subject performed a palm-squeezing task with the right hand following the tact (1.5 Hz) presented by a metronome. One measurement cycle included a 20-s stimulation time and a 20-s resting period. This cycle was repeated 10 times. Before starting the measurement cycles and after finishing all 10 cycles, a 2-min baseline was recorded. Both

protocols were approved by the Institutional Review Board of the University of Illinois at Urbana-Champaign.

### Data Analysis

The raw optical data for AC were converted into values for  $[O_2Hb]$  and  $[HHb]$  using the differential pathlength factor (DPF) method (Delpy *et al.*, 1988; Wray *et al.*, 1988). We chose the AC for the calculation instead of the DC to reduce noise because the AC is not sensitive to ambient light; i.e., we can exclude any direct interference from the light used for the visual stimulation with the reflected light. The values for the DPFs for the adult head of 6.2 at 758 nm and 5.9 at 830 nm were taken from the literature (Duncan *et al.*, 1995) and that of 6.95 at 670 nm from our own measurements (unpublished data). The changes in absorption ( $\Delta\mu_{a \text{ wavelength}}$ ) were converted into changes in  $[O_2Hb]$  and  $[HHb]$  using the equations

Visual cortex:

$$[O_2Hb] = -0.1226 \cdot \Delta\mu_{a \text{ 670 nm}} + 0.4818 \cdot \Delta\mu_{a \text{ 830 nm}}$$

$$[HHb] = 0.1593 \cdot \Delta\mu_{a \text{ 670 nm}} - 0.0674 \cdot \Delta\mu_{a \text{ 830 nm}} \text{ and}$$

Motor cortex:

$$[O_2Hb] = -0.2842 \cdot \Delta\mu_{a \text{ 758 nm}} + 0.6131 \cdot \Delta\mu_{a \text{ 830 nm}}$$

$$[HHb] = 0.3674 \cdot \Delta\mu_{a \text{ 758 nm}} - 0.2342 \cdot \Delta\mu_{a \text{ 830 nm}}.$$

The raw data were recorded at a sample rate of 64 or 80 Hz, which was averaged down to 2.0 or 2.5 Hz to reduce noise for the visual stimulation. It was synchronized to the reversing rate of the stimulation. The sample rate for the motor stimulation was 1.6 Hz. For each location and subject separately, the repeated stimulation periods and resting periods were averaged time locked with respect to the stimulation (folding average). This method removes physiological changes in  $[O_2Hb]$  and  $[HHb]$  due to the heart rate, breathing, or vasomotion which are not associated with neuronal activity. Since the algorithm quantifies relative concentration changes in  $[O_2Hb]$  and  $[HHb]$ ; i.e., the baseline is arbitrary, an offset was added to the  $[O_2Hb]$  and  $[HHb]$  traces to get a zero value instantaneously before the onset of the stimulation. A moving average over five data points was calculated. The  $[HHb]$  trace was compared to the  $[O_2Hb]$  trace using a linear regression.

### Subjects

For the visual stimulation protocol three (two female, one male) and for the motor stimulation protocol four (four male) healthy volunteers with an age range of 18–37 years were included. Written informed con-

sent was obtained from all subjects prior to the experiments.

## RESULTS

### Visual Stimulation

In the visual cortex we found a remarkably strong correlation between the  $[O_2Hb]$  and the  $[HHb]$  patterns (Figs. 2–4). In 13 of a total of 24 locations the correlation coefficient was high ( $r^2 > 0.8$ ). The mean slope of the linear regression, i.e., the scaling factor, between  $[O_2Hb]$  and  $[HHb]$  was  $-3.93 \pm 0.31$  (SE). In 20 locations the change in  $[O_2Hb]$  was larger than  $0.25 \mu M$ .

### Motor Stimulation

The patterns of the  $[O_2Hb]$  and  $[HHb]$  traces are quite different over the motor cortex compared to those over the visual cortex (Figs. 5–7). This is confirmed by the linear regression analysis between  $[O_2Hb]$  and  $[HHb]$ , where in none of the 40 locations (10 locations  $\cdot$  4 subjects) is the  $r^2$  larger than 0.8. The mean slope of the regression line is  $-1.76 \pm 0.20$  (SE). The slopes of the regression lines from the visual cortex are highly significantly lower than those from the motor cortex ( $P < 0.0000001$ ; Mann–Whitney test). In 20 locations the change in  $[O_2Hb]$  is larger than  $0.25 \mu M$ . Detailed data for both cortices are displayed in Table 1.

## DISCUSSION

Our results with regard to the  $[O_2Hb]$  and  $[HHb]$  traces for both the visual and the motor cortices during functional stimulation are consistent with those of other publications (Hirth *et al.*, 1997; Obrig and Villringer, 1997). We will interpret the results of our study on the basis of the one-compartment model described in the Introduction. Increased neuronal activity leads to a higher  $CMRO_2$  (Hoge *et al.*, 1999; Kim *et al.*, 1999). However, we do not see a pattern as in Fig. 1 (middle) (isolated  $CMRO_2$  increase) because the CBF increases immediately after the onset of the stimulation. Our data showed no evidence of a delay between the  $CMRO_2$  and the CBF increases. In other words we did not observe a short increase in  $[HHb]$  appearing at the onset of the stimulation, also known as “dip” (Malonek and Grinvald, 1996). Since the increase in CBF exceeds the increase in  $CMRO_2$ ,  $[O_2Hb]$  increases and  $[HHb]$  decreases. The increase in  $[O_2Hb]$  is larger than the decrease in  $[HHb]$ ; i.e., there is an increase in  $[tHb]$ .

In the visual cortex the increase in the  $[tHb]$  does not perturb the symmetrical pattern of the  $[O_2Hb]$  and  $[HHb]$ ; it causes only a different scaling of  $[O_2Hb]$  and  $[HHb]$ . In contrast, in the motor cortex the symmetry of the  $[O_2Hb]$  and  $[HHb]$  traces is abolished. This leads to

the conclusion that the regulation of the  $[tHb]$  is different in the two cortices.

These differences in the neurovascular coupling between the visual and the motor cortices are further confirmed by the statistics, which show a high correlation coefficient ( $r^2 > 0.8$ ) in more than half of the locations over the visual cortex and in none of the locations over the motor cortex. Furthermore the slopes of the regression line are highly significantly different for the two cortices ( $P < 0.0000001$ ).

To estimate the proportion of the change in  $CMRO_2$  compared to the change in CBF, let us consider the following model. To keep the model simple we initially assume a negligible change in  $CMRO_2$ . Furthermore, we suppose a mean absolute  $[tHb]$  of  $73.8 \mu mol/L$  (Wolf *et al.*, 1997) and a mean CBF of  $46.7 ml/100 g \cdot min$  according to Meltzer *et al.* (2000) ( $59 ml/100 g \cdot min$ ) and Wirestam *et al.* (2000) ( $48$  and  $33 ml/100 g \cdot min$ ), which corresponds approximately to a cerebral hemoglobin flow (CHbF) of  $749.9 \mu mol/min$  (Wolf *et al.*, 1997), mean increases in  $[tHb]$  of  $0.59 \mu mol/L$  during visual and  $0.11 \mu mol/L$  during motor stimulation, and mean decreases in  $[HHb]$  of  $0.23 \mu mol/L$  (visual) and  $0.18 \mu mol/L$  (motor). According to the central volume principle, the mean transit time (MTT) =  $CBV/CBF = tHb/CHbF = 0.098 min$ . During stimulation the increase in  $[tHb]$  corresponds to 0.80% (visual) and 0.15% (motor) compared to the absolute value of the  $[tHb]$  of  $73.8 \mu mol/L$ . Considering that arterial blood is completely oxygenated, we can deduct the change in CHbF from the decrease in  $[HHb]$ , which corresponds to the amount of hemoglobin washed out during a period of one MTT. The CHbF has to be increased exactly by that amount, which leads to an increase in CHbF of 0.31% (visual) and 0.24% (motor). The  $[tHb]$  can increase either by dilation of the blood vessels or by opening of additional blood vessels. The volume of the vessels is  $\pi \cdot r^2 \cdot L \cdot n$ , where  $r$  is the radius,  $L$  is the length of a vessel, and  $n$  is the number of vessels. In the case of dilation the  $r \sim [tHb]^{1/2}$ ; i.e.,  $r$  increases proportionally to the squareroot of the  $[tHb]$ . Thus the radius would increase by 0.40% (visual) and by 0.075% (motor). The resistance of the vessels for a fluid is  $R = (8 \cdot \eta \cdot L)/(\pi \cdot r^4)$ , where  $\eta$  is the viscosity; i.e., the  $R \sim 1/r^4$ . In our case the  $R$  would decrease by 1.6% (visual) or by 0.3% (motor). A decrease in  $R$  would lead to an equal increase in CHbF. This means that for the visual cortex we would expect a four-times-higher increase in CHbF than we have observed. This can be explained by an increase in  $CMRO_2$ , which compensates 3/4 of the decrease in  $[HHb]$  (Fig. 1). For the motor cortex we get approximately the correct change in CHbF, which implies that the  $CMRO_2$  changes little during stimulation.

In the case of additional blood vessels opening up without any change in their diameter, the change in  $R$  will be inversely proportional to the number of blood



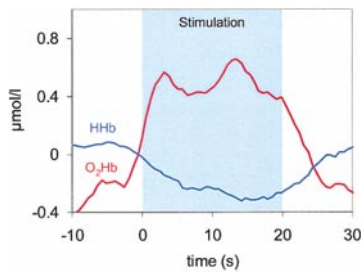


**FIG. 5.** A typical pattern of  $[O_2Hb]$  and  $[HHb]$  during a motor stimulation. The traces represent the folding average over 10 repetitive stimulation periods of location 6 in subject 7. The increase in  $[O_2Hb]$  reaches its maximum much earlier than the decrease in  $[HHb]$  reaches its minimum.

vessels; i.e.,  $R$  decreases by 0.80% (visual) and by 0.15% (motor), which again leads to an equal increase in  $CHbF$ . For the visual cortex we find an increase in  $CHbF$ , which is bigger than the one we actually find. However, for the motor cortex, we would expect from the change in  $[tHb]$  a lower increase in  $CHbF$  than we observe. This can be explained either by a reduction in  $CMRO_2$ , which is very unlikely, or by the fact that the increase in  $[tHb]$  is caused by a dilation of vessels rather than by an opening of additional vessels. Grubb *et al.* (1974) suggested that the change in  $[tHb]$  is coupled to a change in CBF by the equation  $CBV = 0.8 \cdot CBF^{0.38}$ . This type of relation would lead to asym-

metric transients between  $[O_2Hb]$  and  $[HHb]$  traces, particularly shortly after a change in CBF (Fig. 8). In fact any change in  $[tHb]$ , which is directly coupled to CBF, would lead to asymmetric patterns. Grubb *et al.*'s equation is valid only for steady state conditions and not during transients as in our case. The symmetric patterns seen in the visual cortex (Figs. 2–4) are particular. The symmetry can be maintained only if the  $[tHb]$  increase is in exact relation to the proportion of the compartment that has already been washed out. One possibility is that the  $[tHb]$  is related to the oxygenation of the compartment.

The pattern in the motor cortex where the increase in the  $[O_2Hb]$  reaches its maximum faster than the decrease in  $[HHb]$  reaches its minimum can be explained by a decoupling of the  $[tHb]$  increase and the washout. The  $[tHb]$  increases faster than the washout occurs.

We have not used the same sample rates for the visual and motor cortices; i.e., we have more data points for the stimulation and rest periods for the visual cortex than for the motor cortex. A higher number of data points generally reduces  $r^2$  but does not affect the ratio of a linear regression. Thus using the same sample rate would have increased the difference in  $r^2$  between the visual and the motor cortices. It is difficult to compare the signal-to-noise ratio of the measurements between the two cortices, because it depends on

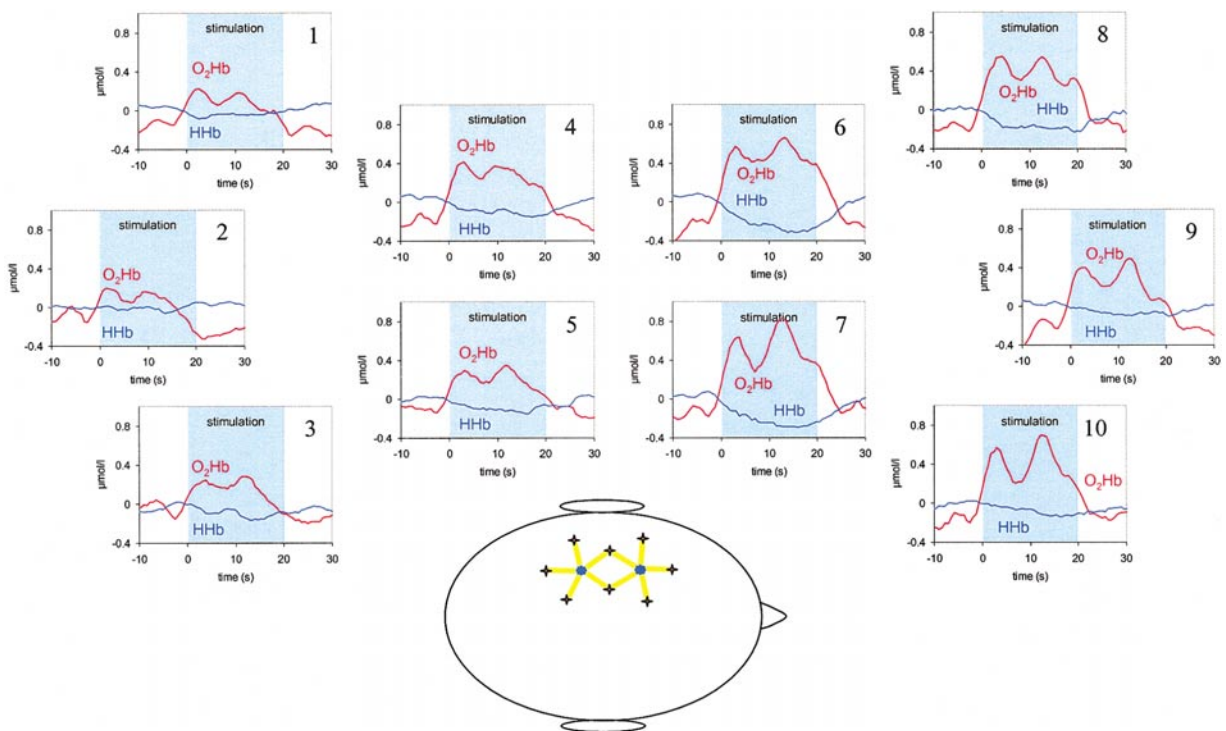


**FIG. 6.** A simultaneously obtained map of the entire region covered by the probe ( $6 \times 9$  cm). The changes in  $[O_2Hb]$  are similar for the entire region. The changes in  $[HHb]$  express more variation depending on the location. The traces represent the folding average over 10 stimulations periods in subject 7.

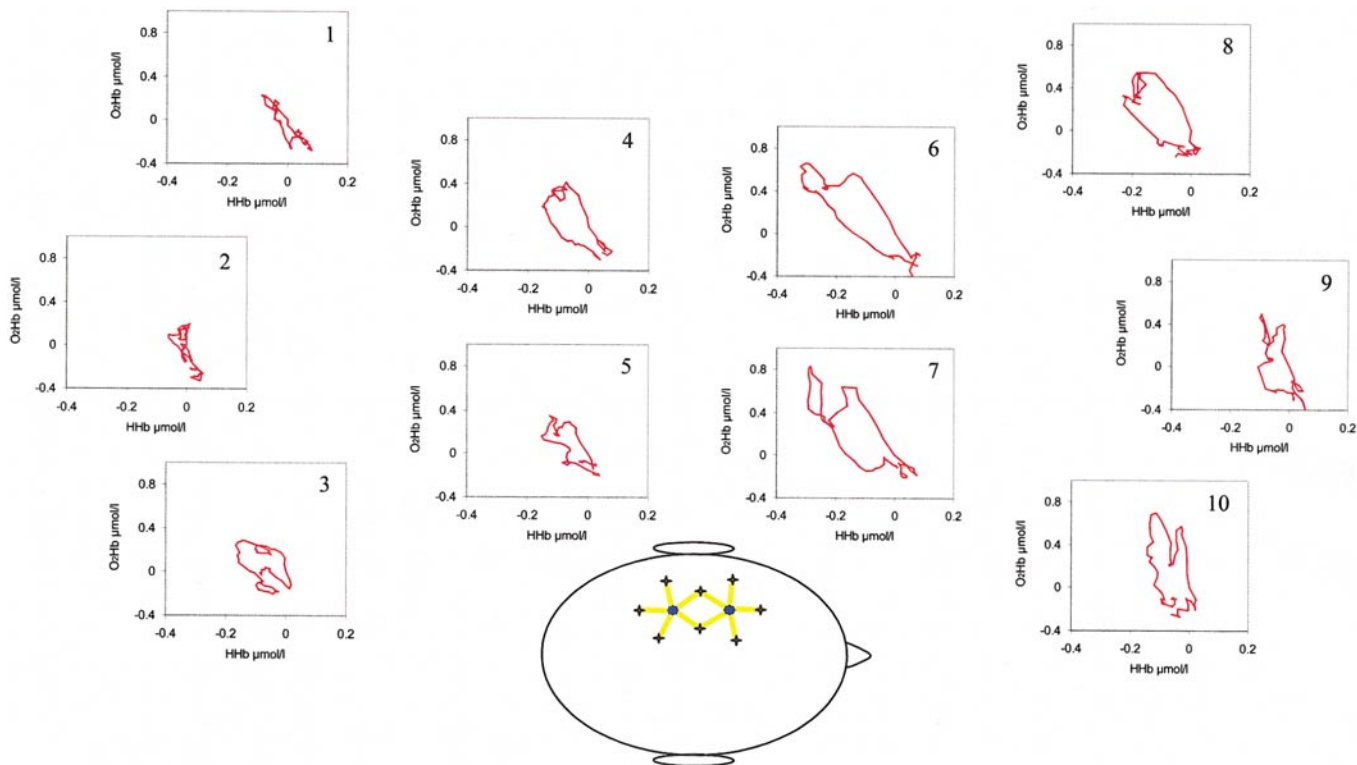


**FIG. 7.** The [HHb] traces were plotted against the [O<sub>2</sub>Hb] traces. The pattern looks very different compared to that for the visual cortex (Fig. 4). The round shape of the pattern indicates a time lag between the two traces. The increase in the [O<sub>2</sub>Hb] reaches its maximum much faster than the decrease in the [HHb] reaches its minimum. Furthermore the [O<sub>2</sub>Hb] returns earlier to the baseline than [HHb].

factors which are difficult to assess, such as the absolute intensity of the detected light, the optical properties of the tissue, and the physiological background noise.

Could the strong correlation between [O<sub>2</sub>Hb] and [HHb] in the visual cortex be due to an artifact? The crossed source detector pairs could be subject to a partial volume effect; i.e., the light bundles are probing different volumes of tissue. This is always the case to some extent, even if the probes are not crossed as in the motor cortex setup, because different wavelengths probe different volumes of tissue. In addition the source detector distance affects the penetration depth of the light bundle. From the diffusion approximation of light transport through tissue, we estimate that the variability in mean penetration depth caused by different source detector distances and different wavelengths are minute (<1 mm). Furthermore, if the strong correlation was caused by a partial volume effect, we would expect different slopes in the regression lines, depending on the location in the map, which is clearly not the case. Furthermore, in every location the raw optical intensities at both wavelengths changed in opposite directions. This excludes many other effects, such as movement artifacts or changes in light scattering, where the intensity at both wavelengths would shift in the same direction. In addition when using a

$\pi$ -sensor on the motor cortex we did not find the strong correlations found for the visual cortex.

Toronov *et al.* (2001) compared simultaneous fNIRS and fMRI measurements during a motor activation task. They found a good temporal correlation and collocation of the changes in [HHb] measured by fNIRS with the BOLD signal measured by fMRI and were able to demonstrate the intracranial origin of the NIRS signal.

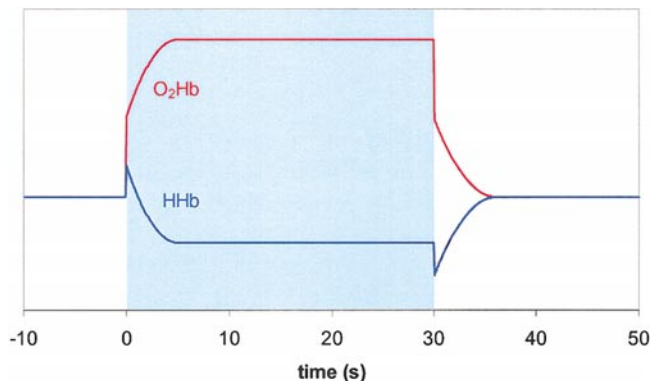


**FIG. 8.** Hypothetical traces of [O<sub>2</sub>Hb] and [HHb] under the assumption of Grubb *et al.* (1974) that total hemoglobin concentration and cerebral blood flow increase simultaneously (shaded area). The pattern exhibits characteristic features which were not found *in vivo*.



**TABLE 1**

Detailed Data of the Response to Visual and Motor Stimulation

Visual cortex						Motor cortex					
Subject	Location	O <sub>2</sub> Hb	HHb	Slope	$r^2$	Subject	Location	O <sub>2</sub> Hb	HHb	Slope	$r^2$
1	1	0.19	-0.08	-1.59	0.17	4	1	0.19	-0.15	-0.53	0.13
1	2	0.69	-0.22	-3.53	0.96	4	2	0.24	-0.17	-0.53	0.05
1	3	0.57	-0.21	-3.15	0.97	4	3	0.16	-0.07	-0.38	0.01
1	4	0.98	-0.35	-3.32	0.93	4	4	0.33	-0.36	-0.85	0.63
1	5	0.07	-0.11	-0.67	0.17	4	5	0.16	-0.08	0.00	0.00
1	6	0.22	-0.21	-1.10	0.90	4	6	0.22	-0.16	-0.81	0.28
1	7	0.28	-0.20	-1.47	0.96	4	7	0.24	-0.12	-0.26	0.01
1	8	0.25	-0.16	-1.25	0.53	4	8	0.07	-0.08	-0.50	0.03
2	1	2.56	-0.56	-4.16	0.98	4	9	0.08	-0.07	-0.45	0.02
2	2	2.63	-0.59	-4.21	0.99	4	10	0.11	-0.05	-1.83	0.44
2	3	2.07	-0.45	-3.97	0.98	5	1	0.47	-0.25	-2.12	0.47
2	4	1.39	-0.33	-4.27	0.98	5	2	0.47	-0.14	-0.94	0.02
2	5	1.32	-0.29	-3.56	0.73	5	3	0.17	-0.36	0.11	0.01
2	6	0.79	-0.17	-3.20	0.64	5	4	0.33	-0.21	-0.90	0.19
2	7	1.23	-0.28	-4.05	0.81	5	5	0.24	-0.22	-0.38	0.02
2	8	0.26	-0.25	-1.12	0.58	5	6	0.20	-0.25	0.57	0.07
3	1	0.79	-0.18	-4.45	0.89	5	7	0.02	-0.11	1.01	0.10
3	2	0.59	-0.20	-3.43	0.88	5	8	0.28	-0.44	0.96	0.43
3	3	0.49	-0.14	-3.72	0.77	5	9	0.11	-0.15	1.44	0.20
3	4	0.74	-0.12	-3.89	0.59	5	10	0.12	-0.17	1.58	0.28
3	5	0.52	-0.12	-4.96	0.82	6	1	0.31	-0.12	-1.95	0.49
3	6	0.36	-0.11	-4.43	0.34	6	2	0.38	-0.12	-3.10	0.51
3	7	0.49	-0.09	-7.81	0.79	6	3	0.26	-0.09	-2.50	0.56
3	8	0.36	-0.10	-5.85	0.49	6	4	0.28	-0.14	-2.49	0.56
						6	5	0.43	-0.13	-2.56	0.58
						6	6	0.41	-0.20	-1.29	0.36
						6	7	0.52	-0.25	-1.92	0.68
						6	8	0.27	-0.11	-1.58	0.37
						6	9	0.24	-0.15	-1.15	0.41
						6	10	0.58	-0.22	-1.94	0.56
						7	1	0.74	-0.23	-1.97	0.15
						7	2	0.08	-0.17	-2.69	0.34
						7	3	0.18	-0.28	-2.17	0.56
						7	4	0.85	-0.37	-2.11	0.67
						7	5	0.55	-0.33	-2.14	0.78
						7	6	0.27	-0.17	-2.05	0.56
						7	7	0.45	-0.23	-2.33	0.55
						7	8	0.30	-0.21	-1.39	0.23
						7	9	0.10	-0.07	-2.69	0.38
						7	10	0.15	-0.09	-2.54	0.70

*Note.* The maximum change in [O<sub>2</sub>Hb], the minimum of the change in [HHb], the slope for the linear regression, and the respective correlation coefficient are given. The location numbers correspond to those depicted in Figs. 3 and 4 or in Figs. 5 and 6.

The [O<sub>2</sub>Hb] signals in the motor cortex have two maxima during the stimulation. This effect has been found previously (Hirth *et al.*, 1997; Obrig and Villringer, 1997; Colier *et al.*, 1999) and appears to be typical for the motor cortex. In Figs. 5 and 6 the [O<sub>2</sub>Hb] starts to increase approximately 2 s prior to the finger-tapping exercise. This effect has been demonstrated previously (Roth *et al.*, 1996; Colier *et al.*, 1999) and is probably due to the mental simulation of movements in anticipation of the exercise. It has been found in 66% of the subjects.

The fact that the patterns are more localized in the visual cortex than in the motor cortex can also be attributed in part to the crossed source detector pair

arrangement, which is expected to give a better spatial resolution (Filiaci *et al.*, 1998).

## CONCLUSION

In the visual cortex the pattern of the [O<sub>2</sub>Hb] is strongly linearly correlated to the pattern of [HHb], which is not the case for the motor cortex. This implies that the regulation of perfusion in the visual cortex is different from that in the motor cortex. There is evidence that the CMRO<sub>2</sub> increases substantially in the visual cortex, while it remains virtually unchanged in the motor cortex.

## ACKNOWLEDGMENTS

This research was supported by NIH Grants PHS 2 ROI CA57032 and RR 10966.

## REFERENCES

- Colier, W. N., Quaresima, V., Oeseburg, B., and Ferrari, M. 1999. Human motor-cortex oxygenation changes induced by cyclic coupled movements of hand and foot. *Exp. Brain Res.* **129**: 457–461.
- Delpy, D. T., Cope, M., van der Zee, P., Arridge, S. R., Wray, S., and Wyatt, J. S. 1988. Estimation of optical pathlength through tissue from direct time of flight measurements. *Phys. Med. Biol.* **33**: 1433–1442.
- Duncan, A., Meek, J. H., Tysczuk, L., Clemente, M., Elwell, C. E., Cope, M., and Delpy, D. T. 1995. Optical pathlength measurements on the adult head, calf and forearm and the head of the newborn infant using phase resolved optical spectroscopy. *Phys. Med. Biol.* **40**: 1–10.
- Fantini, S., Franceschini, M. A., Maier, J. S., Walker, S. A., Barbieri, B., and Gratton, E. 1995. Frequency-domain multichannel optical detector for non-invasive tissue spectroscopy and oximetry. *Opt. Eng.* **34**: 32–42.
- Filiaci, M., Toronov, V., Fantini, S., and Gratton, E. 1998. Optical probe and frequency-domain instrumentation to study spatial and temporal correlation of fluctuations in tissue. *OSA TOPS* **22**: 183–187.
- Frostig, R. D., Lieke, E. E., Ts'o, D. Y., and Grinvald, A. 1990. Cortical functional architecture and local coupling between neuronal activity and the microcirculation revealed by in vivo high-resolution optical imaging of intrinsic signals. *Proc. Natl. Acad. Sci. USA* **87**: 6082–6086.
- Grubb, R. L., Jr., Raichle, M. E., Eichling, J. O., and Ter-Pogossian, M. M. 1974. The effects of changes in PaCO<sub>2</sub> on cerebral blood volume, blood flow, and vascular mean transit time. *Stroke* **5**: 630–639.
- Hirth, C., Villringer, K., Thiel, A., Bernarding, J., Muhlneckl, W., Obrig, H., Dirnagl, U., and Villringer, A. 1997. Toward brain mapping combining near-infrared spectroscopy and high resolution 3D MRI. *Adv. Exp. Med. Biol.* **413**: 139–147.
- Hoge, R. D., Atkinson, J., Gill, B., Crelier, G. R., Marrett, S., and Pike, G. B. 1999. Linear coupling between cerebral blood flow and oxygen consumption in activated human cortex. *Proc. Natl. Acad. Sci. USA* **96**: 9403–9408.
- Hoshi, Y., Onoe, H., Watanabe, Y., Andersson, J., Bergstrom, M., Lilja, A., Langstrom, B., and Tamura, M. 1994. Non-synchronous behavior of neuronal activity, oxidative metabolism and blood supply during mental tasks in man. *Neurosci. Lett.* **172**: 129–133.
- Kato, T., Kamei, A., Takashima, S., and Ozaki, T. 1993. Human visual cortical function during photic stimulation monitoring by means of near-infrared spectroscopy. *J. Cereb. Blood Flow Metab.* **13**: 516–520.
- Kim, S. G., Rostrup, E., Larsson, H. B., Ogawa, S., and Paulson, O. B. 1999. Determination of relative CMRO<sub>2</sub> from CBF and BOLD changes: Significant increase of oxygen consumption rate during visual stimulation. *Magn. Reson. Med.* **41**: 1152–1161.
- Maki, A., Yamashita, Y., Ito, Y., Watanabe, E., Mayanagi, Y., and Koizumi, H. 1995. Spatial and temporal analysis of human motor activity using noninvasive NIR topography. *Med. Phys.* **22**: 1997–2000.
- Malonek, D., and Grinvald, A. 1996. Interactions between electrical activity and cortical microcirculation revealed by imaging spectroscopy: Implications for functional brain mapping. *Science* **272**: 551–554.
- Mayhew, J., Johnston, D., Berwick, J., Jones, M., Coffey, P., and Zheng, Y. 2000. Spectroscopic analysis of neural activity in brain: Increased oxygen consumption following activation of barrel cortex. *NeuroImage* **12**: 664–675.
- Meek, J. H., Elwell, C. E., Khan, M. J., Romaya, J., Wyatt, J. S., Delpy, D. T., and Zeki, S. 1995. Regional changes in haemodynamics as a result of a visual stimulus measured by near infrared spectroscopy. *Proc. R. Soc. Lond. B* **261**: 351–356.
- Meltzer, C. C., Cantwell, M. N., Greer, P. J., Ben-Eliezer, D., Smith, G., Frank, G., Kaye, W. H., Houck, P. R., and Price, J. C. 2000. Does cerebral blood flow decline in healthy aging? A PET study with partial-volume correction. *J. Nucl. Med.* **41**: 1842–1848.
- Obrig, H., and Villringer, A. 1997. Near-infrared spectroscopy in functional activation studies. Can NIRS demonstrate cortical activation? *Adv. Exp. Med. Biol.* **413**: 113–127.
- Roth, M., Decety, J., Raybaudi, M., Massarelli, R., Delon-Martin, C., Segebarth, C., Morand, S., Gemignani, A., Decorps, M., and Jeannerod, M. 1996. Possible involvement of primary motor cortex in mentally simulated movement: A functional magnetic resonance imaging study. *Neuroreport* **7**: 1280–1284.
- Steinmetz, H., Fuerst, G., and Meyer, B. U. 1989. Craniocerebral topography within the international 10–20 system. *Electroencephalogr. Clin. Neurophysiol.* **72**: 499–506.
- Toronov, V., Webb, A., Choi, J. H., Wolf, M., Michalos, A., Gratton, E., and Hueber, D. 2001. Investigation of human brain hemodynamics by simultaneous near-infrared spectroscopy and functional magnetic resonance imaging. *Med. Phys.* **28**: 521–527.
- Villringer, A., and Dirnagl, U. 1995. Coupling of brain activity and cerebral blood flow: Basis of functional neuroimaging. *Cerebrovasc. Brain Metab. Rev.* **7**: 240–276.
- Villringer, A., and Chance, B. 1997. Non-invasive optical spectroscopy and imaging of human brain function. *Trends Neurosci.* **20**: 435–442.
- Wirestam, R., Ryding, E., Lindgren, A., Geijer, B., Holtas, S., and Stahlberg, F. 2000. Absolute cerebral blood flow measured by dynamic susceptibility contrast MRI: A direct comparison with Xe-133 SPECT. *MAGMA* **11**: 96–103.
- Wolf, M., Evans, P., Bucher, H. U., Dietz, V., Keel, M., Strebel, R., and von Siebenthal, K. 1997. Measurement of absolute cerebral haemoglobin concentration in adults and neonates. *Adv. Exp. Med. Biol.* **428**: 219–227.
- Wray, S., Cope, M., Delpy, D. T., Wyatt, J. S., and Reynolds, E. O. 1988. Characterization of the near infrared absorption spectra of cytochrome aa3 and haemoglobin for the non-invasive monitoring of cerebral oxygenation. *Biochim. Biophys. Acta* **933**: 184–192.